Absolute luminescence efficiency of ion-bombarded solid argon

D. E. Grosjean,* R. A. Vidal,† and R. A. Baragiola
Laboratory for Atomic and Surface Physics, Engineering Physics, University of Virginia, Charlottesville, Virginia 22901

W. L. Brown
Bell Laboratories, Lucent Technologies, Murray Hill, New Jersey 07974

(Received 27 January 1997)

We have directly measured the absolute efficiency of the 9.8-eV *M*-band luminescence from the decay of Ar_2* excimers in solid Ar bombarded by 1.5-MeV He^+ and 10–50-keV H^+ ions. About 54% of the electronic energy deposited by the projectiles is converted to 9.8-eV luminescence energy, or about 5.5 photons per 100-eV deposited. The efficiency is also found to be independent of ion and ion energy for those tested over a range of stopping cross sections from 6.5 to 400 eV/(10^{15} atoms/cm^2). This work clearly establishes the *M* band as the major relaxation pathway for electronically deposited energy in solid Ar, a pathway that is an important source of radiation damage and sputtering and which can be affected by electron emission. [S0163-1829(97)00535-3]

I. INTRODUCTION

Luminescence from ion-bombarded rare-gas solids and liquids exhibits a rich spectrum dominated by the copious *M*-band peaking at 9.8 eV, resulting from the decay of molecular excimers. The efficiency of *M*-band luminescence, together with a low Fano factor for good energy resolution, makes rare-gas liquids effective scintillator detectors for ionizing nuclear particles.[1] The high luminescence efficiency also underlies the proposed used of rare-gas solids for lasers in the vacuum ultraviolet.[2–4]

More fundamentally, however, luminescence provides important information about energy pathways for relaxation of electronically deposited energy. While each feature in the luminescence spectrum arises from a different process, the *M* band is particularly significant because of its relation to such other observable processes as sputtering and electron emission.[5–7] However, because luminescence was determined in relative units in previous studies, it was not possible to ascertain whether that luminescence was an important precursor to sputtering from only the correlation of *M*-band luminescence and sputtering yields. For this reason, we have made careful measurements of the *absolute M*-band luminescence yields for solid Ar films under energetic ion bombardment. Results of these studies will serve to ascertain the importance of this energy pathway and should also be applicable to understanding radiation effects in other insulators. Rare-gas solids were chosen as a model system since their electronic states are well known, and since the weak van der Waals bonding allows these monoatomic solids to be treated as dense gases with generally negligible chemical activity in the ground state.[8,9] Furthermore, the use of ion beams allows these measurements to be made over a wide range of electronic energy deposition rates.

To assess the significance of the *M* band, it is important to understand the energy pathways involved. The sequence of events is described by the following well-known model[5,10] (refer to Fig. 1). When solid Ar is bombarded by ionizing particles, such as keV or MeV ions, electronic energy is deposited in the form of electron-hole pairs and direct excitations (excitons). The atomic holes and excitons diffuse primarily by resonant electron transfer processes. A hole can strongly attract a ground-state atom, trap by a structural relaxation assisted by lattice vibrations, and form the Ar_2^+ dimer hole in 10^{-12}–10^{-11} s. The mobility of this dimer is much lower than the hole from which it was formed. After electrons have slowed down sufficiently, in a time of about 10^{-10} s,[11] they can recombine with the Ar_2^+ producing an

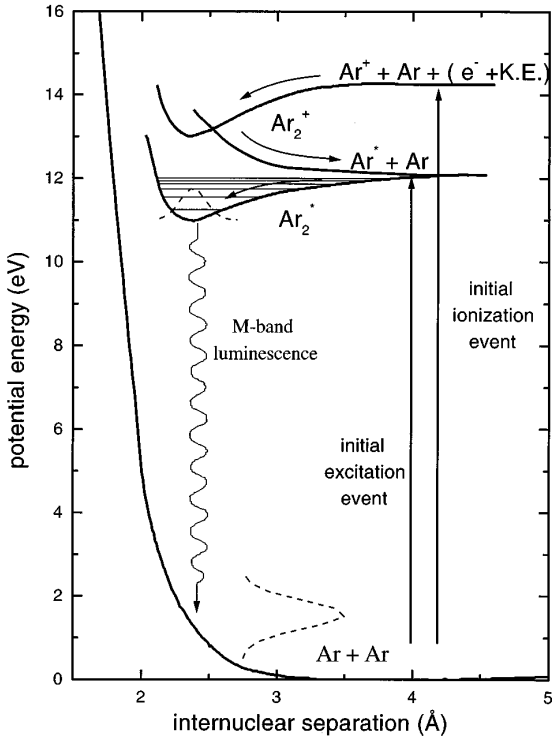

FIG. 1. Ar-Ar potential-energy curves in the solid state. The arrows indicate decay sequences. The decay of the Ar_2* gives rise to the *M* band.

excited Ar atom (Ar*), a ground-state Ar atom, and kinetic energy. If this recombination occurs near the surface, it can produce sputtering of the Ar or Ar* involved, or even of neighboring atoms struck by the separating pair. Excitations (Ar*) can also be produced directly by the projectile or by its associated electronic collision cascade or by Auger recombination of a hole and electron.[12] Regardless of how an Ar* is formed, it can pair with a neighboring ground-state atom in an attractive or repulsive state. If the interaction is a repulsive state and at the surface, the excited Ar* can desorb by cavity ejection.[13] In the attractive state, Ar* combines with a neighbor, again assisted by lattice vibrations, to form the Ar_2* excimer. The vibrationally relaxed Ar_2* excimer will then decay by emission of a 9.8 eV M-band photon to the repulsive part of the ground state of Ar_2 in $\sim 3\times 10^{-9}$ s or 1.4 μs for the $^1\Sigma$ and $^3\Sigma$ excimer states, respectively.[14] The kinetic energy released in this decay can also result in sputtering if the decay occurs close to the surface. A distribution of internuclear distances in the ground state of the Ar_2* well gives rise to the width of the M band and contributes to the distribution of kinetic energies of sputtered atoms (dotted Gaussian curves on Fig. 1).

Several studies of solid argon have shown that luminescence and sputtering correlate with the electronic stopping power of the projectile.[5,15–17] There have been extensive studies,[7,18–20] of the anticorrelation of M-band luminescence and charge collection (separation) in *liquid* Ar bombarded by fast particles which have quantified the contributions of excitation and ionization to M-band luminescence. We have recently reported[6] similar work on solid Ar where the M-band luminescence, charge collection, and sputtering were measured simultaneously. The interplay of these processes gives insight into the energy pathways involved and underscores the importance of having a measurement of the absolute M-band luminescence efficiency which can then quantify the importance of the energy pathway described above.

II. EXPERIMENTS

The experiments were carried out at both the University of Virginia and Bell Laboratories, Lucent Technologies under UHV conditions (about 1×10^{-10} Torr at the target) using 10–50 keV H^+ and 0.5–1.5 MeV H^+, He^+, and Ne^+, respectively, at incident ion fluxes of $(2\times 4)\times 10^{11}$ ions/cm^2 s. Since both experimental setups were very similar, a composite one is shown in Fig. 2 (see Ref. 21 for details of the differences). Argon films were grown by vapor deposition of 99.9995% pure Ar onto a substrate mounted on the rotatable cryostat. The gas manifold at Virginia additionally had an absorption getter pump to further purity the Ar, making the Ar used at Virginia purer than in previous studies. The substrate at Virginia was an optically flat gold coated quartz crystal microbalance cooled to 6–15 K, while at Bell two mirrorlike substrates cooled to 8 K were used: a Si wafer with its native oxide and a Si wafer with a 750-Å gold coating. Gold substrates were chosen because their UV reflectance is very stable over time in air and vacuum.[22] At these temperatures, the vapor pressure of solid Ar is less than 10^{-13} Torr and is therefore negligible; cleanliness of the Ar surface is maintained by the sputtering induced by the ion beam.

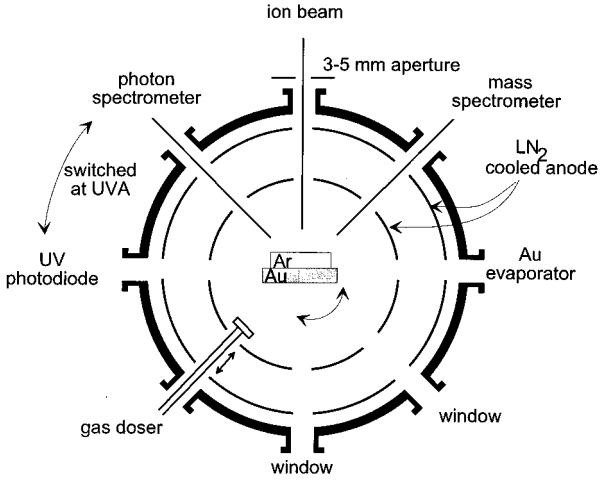

FIG. 2. Composition drawing of the experimental setups at Virginia and at Bell Labs. The UV photodiode occupied different ports relative to the ion beam at the two labs.

The Ar films were grown quickly (about 1000 Å/min) and without interruption and are thus expected to be polycrystalline.[23] Surrounding the target was a cylinder cooled to liquid-nitrogen temperatures which was used for additional pumping. By biasing the cylinder negatively with respect to the target, it also served to suppress the escape of secondary electrons from the Ar film. In all the measurements reported here, the cylinder surrounding the sample was biased negatively with respect to the target holder to prevent secondary electrons from leaving the Ar film. This is important since ejected electrons reduce luminescence by inhibiting the recombination channel.[6] The UV photodiode, used to measure the absolute M-band luminescence efficiency, was calibrated by VUV associates with an uncertainty of 20%.[24] An ultraviolet spectrometer also detects the 9.8-eV photons emitted from the Ar films. The spectrometer at Virginia had a photomultiplier with a sodium salycilate coating which detects visible and VUV photons; the efficiency of the spectrometer without the photomultiplier was calibrated at National Institute of Standards and Technology.[24] The spectrometer at Bell Labs had a channeltron electron multiplier detector, sensitive only to VUV photons.

Typical Ar luminescence spectra, taken at a resolution of 20 Å, are shown in Fig. 3. The main spectrum in Fig. 3 shows the UV features induced by 2-MeV He^+ bombardment. The W band at 11.3 eV has been shown[13,25] to be from sputtered, vibrationally excited $Ar_2^\dagger$ dimers and to be proportional to overall sputtering. The lines at 11.83 eV (1048 Å) and 11.62 eV (1067 Å) are interpreted to be due to sputtered singlet $^1P_1$ and triplet $^3P_1$ Ar*, respectively.[13] Finally there is a line at 11.58 eV (1071 Å) attributed to the decay of an Ar* trapped in the argon lattice, i.e., an atomic self-trapped exciton (a-STE);[26,28] in this spectrum, the triplet and a-STE are not resolved. This singlet, triplet, and W-band features are surface phenomena, while the a-STE and M band are bulk phenomena.[13,25,27] The M-band dominates the luminescence spectrum with an intensity higher than that of the other

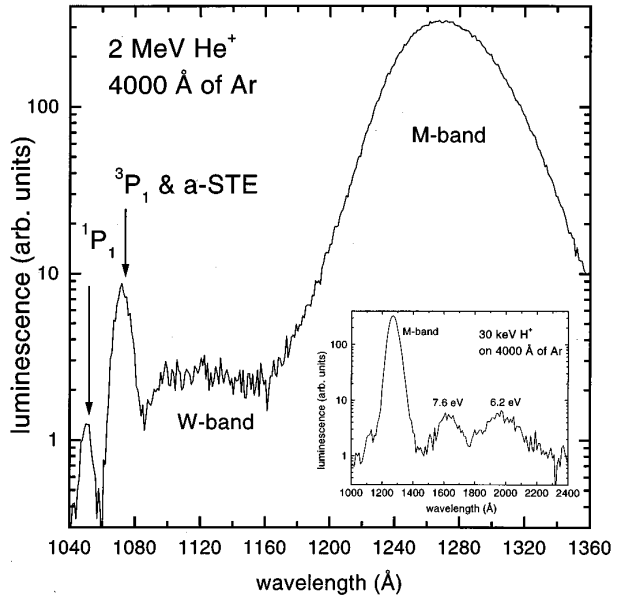

FIG. 3. UV luminescence spectrum of a 4000-Å solid Ar film bombarded by 2-MeV He^+. The inset shows a spectrum produced by 30-keV H^+ on a 4000-Å Ar film that includes lower-energy features. No luminescence features were seen in the range of 2200–5000 Å.

peaks by orders of magnitude. This means that the contribution of the other peaks can be neglected when using the photodiode, even though its efficiency increases by a factor of two in the wavelength region of the atomic features. Any features at wavelengths greater than 1500 Å can also be neglected since the photodiode efficiency becomes negligible for energies less than 8 eV.

The inset of Fig. 3 shows UV and visible features induced by 30-keV H^+ corrected for the efficiency of the spectrometer (no differences in the spectra were seen for different energies of H^+ from 10–50 keV). Three features are apparent in the spectrum at 1265 Å (9.8 eV), 1650 Å (7.6 eV), and 2000 Å (6.2 eV); no other features were seen out to 5000 Å. Similar spectra induced by ion bombardment were measured by Busch *et al.*[2] and Riemann, Brown, and Johnson.[5] These latter authors attributed the features at 7.6 eV and 6.2 eV to N_2 and O_2 impurities,[29] respectively. Langhoff[30] and Grigorashchenko *et al.*,[31] however, attribute the 6.2-eV feature, the so-called ''third continuum'' in the gas phase, to the decay of $(Ar^{2+}Ar)$ to the repulsive ground state of $Ar^+ + Ar^+$. An alternative explanation is the breakup of impurity water molecules in the film, giving rise to Ar_2O and Ar_2H lines at 6.2 and 7.5 eV reported by Kraas and Gürtler.[32] Regardless of the origin of these low-energy features, the 9.8-eV feature clearly dominates, accounting for 94% of the energy in this spectrum.

III. CALCULATION OF ABSOLUTE EFFICIENCY

We determined that the response of the photodiode is directly proportional to the ion-beam current from 0.15 to 400 nA. If I_d is the current measured on the photodiode and q is the elementary charge, then the photon flux measured by the photodiode is given by

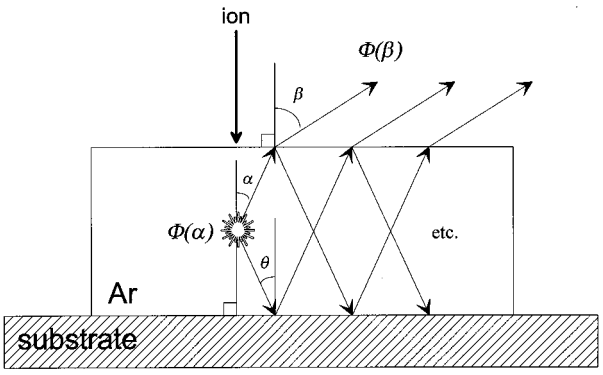

FIG. 4. Geometry for absolute luminescence determination assuming specular reflection at the substrate.

$$\frac{I_d}{q\overline{f}} = \int_\Omega \Phi(\beta)\, d\Omega, \tag{1}$$

where Ω is the solid angle seen by the photodiode, $\Phi(\beta)$ is the angular distribution of the luminescence emitted into vacuum, and $\overline{f} = 0.017$ is the weighted average efficiency of the photodiode over the M band.

We assume that the initial distribution of luminescence emission from each source inside the film is unpolarized and isotropic:

$$\Phi(\alpha) = \frac{I_0}{4\pi}, \tag{2}$$

where I_0 is the total number of photons created inside the film per second. Self-absorption and scattering within the film are neglected; refraction at the Ar/vacuum interface modifies the external emission distribution and makes $\Phi(\beta)$ anisotropic. Here we assume that the films are flat and smooth. If $\Phi(\alpha)$ represents the internal emission distribution (see Fig. 4), then $\Phi(\alpha)\sin\alpha\, d\alpha = \Phi(\beta)\sin\beta\, d\beta$, assuming there are no reflection losses or multiple reflection gains that need to be included. Using Snell's law as well as its differential form, we solve for

$$\Phi(\beta) = \frac{\cos\beta}{n\sqrt{n^2 - \sin^2\beta}}\Phi(\alpha)\,\xi \tag{3}$$

where $n = 1.48$ is the index of refraction for 10-eV photons in solid Ar (Ref. 33) and ξ is a unitless factor that accounts for substrate reflectivity and surface reflections. These will be discussed in the paragraphs below. This expression is valid with the assumption that the film surface is flat on a spatial scale larger than the wavelength of 9.8-eV light.

Part of the luminescence will reflect from the substrate and reach the surface of the film. The substrates had a mirrorlike finish and are thus assumed to reflect specularly. The fraction of the light reflecting from the substrate is $R(\theta)$, the reflectance of the substrate for an incidence angle θ, where $\theta = \alpha$. For 10-eV photons, $R_{Au}(0) = 0.15$ and $R_{Si}(0) \approx 0.3$ for Si with an oxide layer (see the appendix for details of how these values were obtained). The fraction of light (unpolar-

ized) reflected at the Ar/vacuum interface, given by the Fresnel formula $R_{\rm surf}=[(n-1)/(n+1)]^2=0.037$, is rather small. This is approximately constant up to the angle of total internal reflection derived from Snell's law: $\alpha_c=\sin^{-1}(1/n)=42.5°$. The transmittance of the surface is thus $T_{\rm surf}=1-R_{\rm surf}=0.963$.

The fraction of $\Phi(\alpha)$ escaping through the front of the film ξ is then the sum of the light rays and associated reflections that are initially directed towards the surface, and the light rays and associated reflections that are initially directed towards the substrate, giving

$$\xi=T_{\rm surf}\left(\frac{1+R(\theta)}{1-R(\theta)R_{\rm surf}}\right), \tag{4}$$

(see the Appendix for this derivation). Interference effects were not clearly observed in this study, but they must be less than the spread of the data in the thickness dependence of the M band, or about 4%,[12] and therefore have been neglected. Substituting Eqs. (2), (3), and (4) into Eq. (1), and solving for I_0 yields

$$I_0=\frac{4\pi I_d}{qf}\left[\int_\Omega \frac{\cos\beta}{\sqrt{n^2-\sin^2\beta}}T_{\rm surf}\left(\frac{1+R(\theta)}{1-R(\theta)R_{\rm surf}}\right)d\Omega\right]^{-1}. \tag{5}$$

The total-energy efficiency η of the 9.8-eV luminescence, i.e., the fraction of the electronically deposited energy per second P that is converted to M-band luminescence, is given by

$$\eta=\frac{I_0\hbar\omega}{P}, \tag{6}$$

where $\hbar\omega=9.8$ eV per photon. For MeV ions, the amount of energy deposited in the film per second is

$$P=\frac{\overline{S_e}d}{N\cos\theta_B}\frac{I_B}{q},$$

where $\overline{S_e}$ is the average stopping cross section of the incident particle; d is the film thickness; N the number density of solid Ar (2.66×10^{22} atoms/cm^3); θ_B is the angle the ion beam makes with the normal to the surface of the Ar film; and I_B is the ion-beam current. For the thin films used in this work, $S_e\approx S_e(E_0)$, i.e., the projectile energy, projectile trajectory, and S_e do not change significantly as the projectile passes through the film. However, for keV particles and the 12 000-Å films used with them, the projectiles stop in the film making P be determined by the projectile energy minus small corrections due to backscattering and energy loss in elastic collisions. Monte Carlo simulations[34] were used to determine these corrections and derive the amount of *electronic* energy deposited by each particle. Energy deposited within $l\approx200$ Å from the substrate, the diffusion length of holes, is effectively quenched by electron transfer processes with the substrate and does not give rise to 9.8-eV luminescence.[5] This is taken into account by using only the energy deposited in a layer of thickness $d-l$. For the 4000-Å films used with MeV projectiles, this correction amounts to 5%, while for the keV projectiles and thick films, it is less than 0.3%, since most ions deposit their energy far away from the substrate.

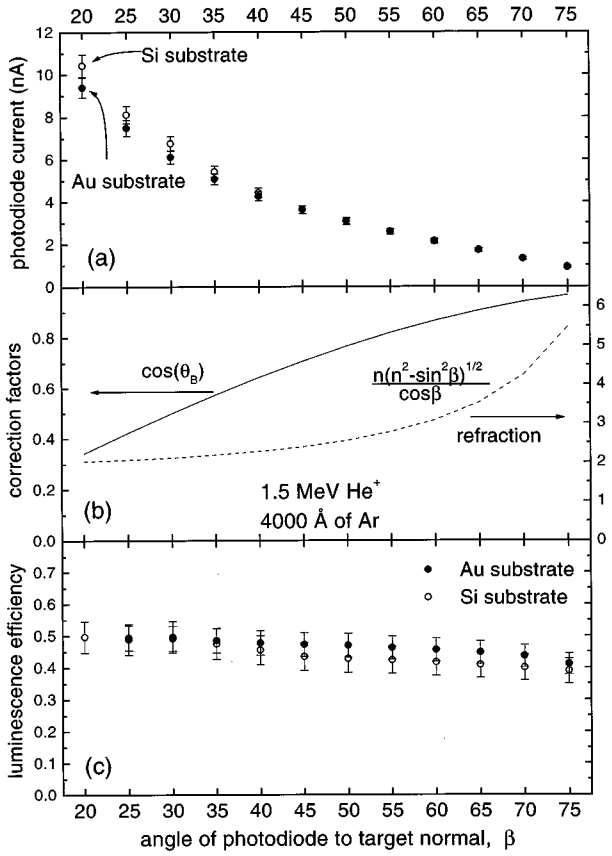

FIG. 5. Absolute luminescence efficiency for M-band luminescence as a function of angle for 1.5-MeV He^+ bombardment. The beam current is 103 nA. There is an additional 20% uncertainty in the calibration of the UV photodiode. (a) raw data, (b) angle dependent corrections applied to the raw data, (c) absolute luminescence efficiency.

IV. RESULTS AND DISCUSSION

Figure 5(a) shows the MeV ion-induced luminescence (photocurrent measured by the UV photodiode) as a function of the angle of observation with respect to the target normal for both Au and Si substrates. Figure 5(b) shows the corrections applied to the data to account for different projectile path lengths (and thus amounts of energy deposited in the film) and to account for refraction at the Ar/vacuum interface. Finally, Fig. 5(c) shows the absolute luminescence efficiency as evaluated using Eq. (6). The incidence angle and refraction corrections appear to account for most of the angular dependence; effects such as ions backscattering into the photodetector and energy not deposited as electronic energy are negligible for MeV He^+. The difference in efficiency of the Au substrate and Si substrate can be accounted for by a lower reflectivity of the Si substrate. The reflectivity of Si decreases as an oxide layer grows,[35] and the oxide layer on the Si substrate used here was not well characterized. We thus use the data taken with the Au substrate and small angles for determining the energy efficiency of MeV par-

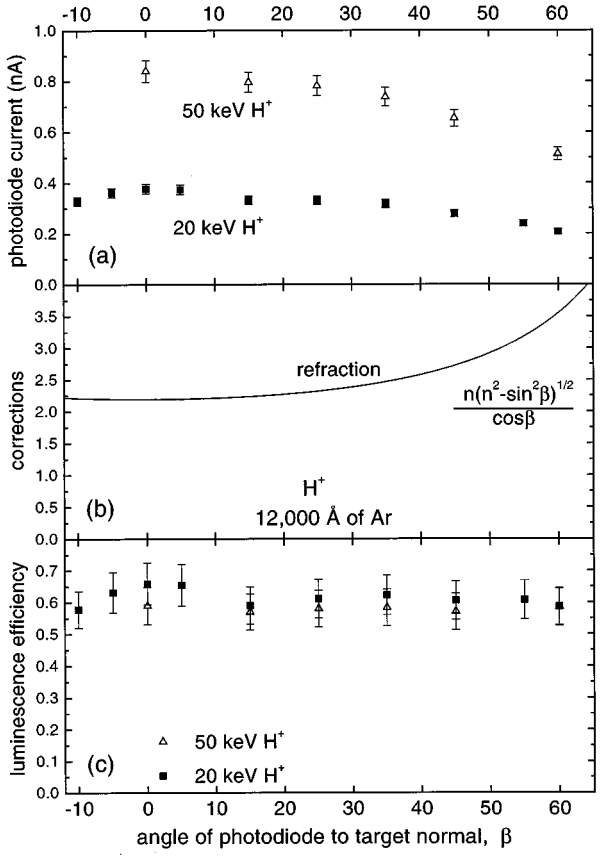

FIG. 6. Absolute luminescence efficiency for M-band luminescence as a function of angle for 20 and 50-keV H^+ bombardment. The beam current is 10 nA. There is an additional 20% uncertainty in the calibration of the UV photodiode. (a) raw data, (b) angle dependent corrections applied to the raw data, (c) absolute luminescence efficiency.

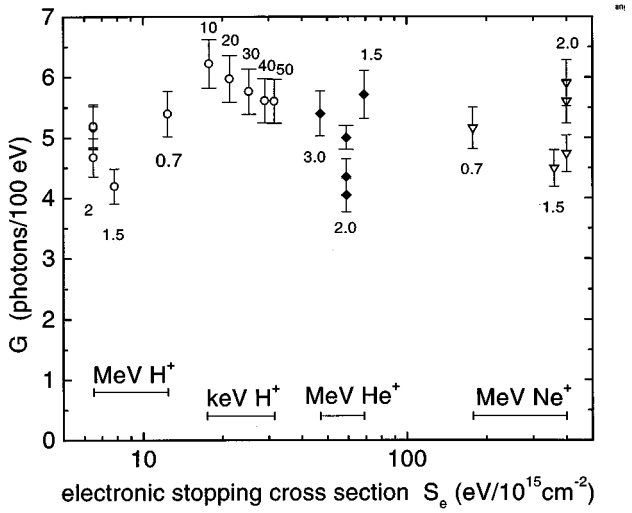

FIG. 7. G, number of M-band photons produced per 100-eV deposited energy as a function of electronic stopping cross section. The numbers near the data points are the energies of the projectiles in the units at the bottom of the graph. There is an additional 20% uncertainty in the calibration of the UV photodiode.

ticles: $\eta=0.49\pm0.10$, where the error is dominated by the uncertainty in the calibration of the photodiode.

The angular dependences of 9.8-eV luminescence (photocurrent measured by the UV photodiode) induced by 20–50 keV protons are measured for 12 000-Å films which are thick enough to stop the incident ions in the films. They are shown in Fig. 6(a), together with the angle correction due to refraction in Fig. 6(b), and the resulting luminescence efficiency in Fig. 6(c). Not shown in Fig. 6(b) are small corrections, evaluated using a Monte Carlo simulation,[34] to account for ions backscattered into the detector (1.7% and 0.2% for 20- and 50-keV H^+, respectively), as well as a correction for energy not deposited electronically in the film—either reflected back into the vacuum or going into elastic collisions (2.4% and 1.1% for 20 and 50-keV H^+, respectively). The corrections for the keV data seem to effectively remove the angular dependence for the calculation of the absolute luminescence efficiency although a small but reproducible ''bump'' near zero degrees remains in the data taken at the lower energies. The calculated efficiencies go from $\eta=0.65$ at 10.1 keV to $\eta=0.57$ at 50.1 keV, averaging $\eta=0.59\pm0.12$ where the error includes the uncertainty in the calibration of the photodiode. These values are close to but slightly higher than the values measured for MeV projectiles, which is possibly due to a purer Ar used in the keV experiments. Because of this small dependence on energy we average the keV and MeV values to conclude that the experiments give a value for Ar luminescence efficiency of $\eta=0.54\pm0.12$. The measured luminescence efficiencies are consistent with ≈0.50, the estimate of Huber, Emmons, and Lerner[28] for the 9.8-eV luminescence efficiency of solid Ar bombarded by 10–30 keV electrons. Our values are higher than gas-phase values: Stewart *et al.*[36] measured $\eta\approx0.29$ for Ar gas at 400-Torr bombarded by 4-MeV protons.

From the value of the energy efficiency extracted above we can obtain the G value for the photon producing process. (The G value is a quantity often used in radiation physics. It is the number of reaction products of a particular kind, in our case 9.8-eV photons, produced per 100 eV of energy deposited.) With an energy efficiency of 0.54 ± 0.12, 5.5 ± 0.8 photons are produced for each 100 eV of electronic excitation. Another quantity, W_S, can also be evaluated: the average energy spent per luminescence decay. W_S has a value of 18.1 ± 3.3 eV. Note that this is less than W, the mean energy spent per ionization, which has a value of[9] 27 ± 1 eV. This difference is due to the fact that in W_S direct excitations lead to photon emission, whereas in W direct excitations are energy that is lost (not used for ionization).

From our data taken over a range of particles and energies we can deduce G as a function of electronic stopping cross section. For MeV ions we have used data taken for 1000-Å Ar films collected by the spectrometer and normalized by the absolute luminescence efficiency determined by the UV photodiode. The values are normalized to the data measured for 2-MeV He^+ at $S_e=59$ eV/$(10^{15}/\mathrm{cm}^2)$.[34] For keV protons, we did not use thin films to determine G because of the uncertainty in the S_e needed to obtain the energy deposited in the films. Rather, we used the UV photodiode to measure light emission from films thicker than the range of the ions and derived the total number of photons excited in the film per incident ion, $L(E)$. Then, $G(E)=0.1[dL(E)/dE]$ follows from the definition of G if the energy is given in keV.

We approximate this differential by using luminescence data at two energies, $E+\Delta E$ and $E-\Delta E$: $G(E)=0.1[L(E+\Delta E)-L(E-\Delta E)]/2\Delta E$, where E and ΔE are in keV.

The quantity G is plotted in Fig. 7 for a wide range of S_e and has an average value of 5.4 ± 1.1 photons/100 eV. The values for MeV H^+ and MeV Ne^+ incident ions were measured using the UV spectrometer and normalized to the UV spectrometer signal for the MeV He^+ measurements, from which we then normalized to the luminescence efficiency of MeV He^+. Angular dependences of the luminescence efficiency were not performed for the MeV H^+ and MeV Ne^+ projectiles. The lack of any trend in these data indicates that direct proportionality between the luminescence and S_e continues up to $S_e=400$ eV/$(10^{15}/\mathrm{cm}^2)$. According to Hitachi, Doke, and Mozumder[18] the proportionality breaks down for high excitation densities occurring at $S_e>600$ eV/$(10^{15}/\mathrm{cm}^2)$, where excitation may be quenched by biexcitonic mechanisms such as $X^*+X^*\rightarrow X^++X+e^-$.

Using the (energy) luminescence efficiency, the quantum efficiency of an ionization leading to a 9.8-eV photon can be approximated. In addition to ionizations, the ion-beam creates direct excitations which can also lead to luminescence and which can account for up to 35% of the total 9.8-eV luminescence for 2-MeV H^+ bombardment.[6] For each 100 eV of energy deposited by the fast protons, our results show that 49 ± 12 eV goes into 9.8 eV photons, corresponding to 5 ± 1 photons. As mentioned, 35% of the luminescence (1.75 ± 0.04 photons) or of the energy (17.2 ± 0.3 eV) is from direct excitations, and thus 3.3 ± 0.7 photons are from the decay of excited states originating in ionizations. We compare this number to that of excited states which result when electrons and holes recombine. For a W value of 27 ± 1 eV, 3.70 ± 0.14 electron-hole pairs are produced for 100 eV of deposited energy. This gives a quantum efficiency of 0.9 ± 0.2 for conversion of holes to 9.8-eV photons. This value is consistent, within uncertainties, with a value of 1 that would be expected if the M-band transition were the only pathway to the ground state, in the absence of impurities. This result is thus significant for establishing the dominance of the M-band pathway.

The M-band luminescence efficiency has been seen to be dependent on irradiation dose.[37,21] Reimann observed that, using the known absolute sputtering yield, the M-band luminescence intensity decreases faster than would be expected for 1.5-MeV He^+ bombardment, based on the thickness dependence of the luminescence measured from fresher films.[37] In this work, we observed the same effect for 2-MeV Ne^+: after measuring a 10% decrease in film thickness due to sputtering, luminescence decreased by 75%, indicating that luminescence *efficiency* actually decreased. We did not observe this effect for MeV H^+ even for doses as high as 5×10^{15} H^+/cm^2, suggesting that damage (or formation of quenching centers) correlated with stopping cross section is responsible for decreasing the luminescence efficiency, though the reason for this efficiency decrease is not understood. The luminescence efficiency measurements made in this work were done for doses that did not show a measurable efficiency decrease.

In summary, it has been shown that the conversion of electronically deposited energy in solid Ar films to 9.8-eV luminescence is quite efficient, ≈54% for ion bombardment at both MeV and keV energies. This corresponds to a G value of 5.5 photons/100 eV of electronic energy deposited which was shown to be roughly constant over a stopping cross section range of 6.5–400 eV/$(10^{15}/\mathrm{cm}^2)$. From the energy efficiency, a quantum efficiency for the conversion of holes to 9.8-eV photons was calculated to be near unity. Clearly, the M band in solid Ar is the major energy pathway for electronically deposited energy. This pathways is furthermore significant because it is an important source of radiation damage and sputtering, and because energy can be diverted away from it by inducing electron emission (preventing recombination).

ACKNOWLEDGMENTS

This work was partially supported by the National Science Foundation through Grant No. DMR-9121272. R.V. acknowledges support from the Conseguo Nacional de Investigaciones Científicas y Técnicas of Argentina and from Fundación Antorchas. We are grateful to R. E. Johnson for stimulating discussions, and to M. S. Westley and F. C. Unterwald for valuable technical assistance.

APPENDIX

Here we describe various details of the absolute luminescence efficiency calculation, including the evaluation of the substrate reflectivity and the summation of internal reflections. The reflectivity of the substrate as a function of incidence angle, $R(\theta)$, is important in the calculation of the absolute luminescence yield. Its effect on the observed light intensity was evaluated using standard equations for reflection and refraction at interfaces[38] and compared with experimental measurements. The reflectivity of the Au/vacuum interface for 9.8-eV photons at normal incidence was calculated using $n_{\mathrm{Au}}=1.187$ and $k_{\mathrm{Au}}=1.070$,[39] where n_{Au} and k_{Au} are the refractive index and extinction coefficient of Au, respectively. This yields a value of 19.9%, very close to the experimental measurement of 19.7%.[40] The reflectance was then calculated for an Ar/gold interface as a function of incident angle, using $n_{\mathrm{Ar}}=1.48$ and $k_{\mathrm{Ar}}=0$.[33] The average of the parallel and perpendicular polarization was used for the absolute luminescence calculations because the light is not known to be polarized. Nevertheless, the effect on the absolute luminescence calculation of differently polarized light reflecting from the Ar/Au interface amounted to less than 5%. The reflectance is quite flat for incident angles from 0 to 42.5°, the angle of total internal reflection, and it has a value of 0.15.

For the evaluation of luminescence of films deposited on a Si substrate, we did not calculate the reflectance versus angle of incidence since this substrate was not well characterized. The reflectance was taken to be independent of angle from 0 to 42.5°, based on the results for the Ar/Au interface, and equal to about 30% based on published measurements that discuss the effect of an oxide layer on Si.[35]

Calculating the fraction of $\Phi(\alpha)$ that escapes through the front of the film ξ for a specularly reflecting substrate involves evaluating the sum of the light rays and associated reflections that are initially directed towards the surface,

$$\xi_1=T_{\mathrm{surf}}[1+R(\theta)R_{\mathrm{surf}}+(R(\theta)R_{\mathrm{surf}})^2+\cdots]$$

and the light rays and associated reflections that are initially directed towards the substrate,

$$\xi_2 = T_{\text{surf}} R(\theta)[1 + R(\theta) R_{\text{surf}} + (R(\theta) R_{\text{surf}})^2 + \cdots]$$

(see Fig. 4). Using the infinite sum

$$\sum_{k=0}^{\infty} a q^k = \frac{a}{1-q}$$

for $|q| < 1$, we evaluate $\xi_1 + \xi_2$ to get

$$\xi = \xi_1 + \xi_2 = T_{\text{surf}} \left(\frac{1 + R(\theta)}{1 - R(\theta) R_{\text{surf}}} \right),$$

which is [Eq. (4)].

*Also at Bell Laboratories, Lucent Technologies, Murray Hill, NJ 07974. Present address: NEC Corporation, 34 Miyukigaoka, Tsukuba, Ibaraki 305, Japan.

†Permanent address: INTEC, Güemes 3450, 3000 Santa Fe, Argentina.

[1] T. Doke, Port. Phys. **12**, 9 (1981).

[2] B. Busch, A. Ulrich, W. Krötz, and G. Ribitzki, Appl. Phys. Lett. **53**, 1172 (1988).

[3] H. Nahme and N. Schwentner, Appl. Phys. B **51**, 191 (1990).

[4] G. Schilling, W. E. Ernst, and N. Schwentner, IEEE J. Quantum Electron. **29**, 2702 (1993).

[5] C. T. Riemann, W. L. Brown, and R. E. Johnson, Phys. Rev. B **37**, 1455 (1988).

[6] D. E. Grosjean, R. A. Baragiola, and W. L. Brown, Phys. Rev. Lett. **74**, 1474 (1995).

[7] S. Kubota, A. Nakamoto, T. Takahashi, E. Shibamura, M. Miyajima, K. Masuda, and T. Doke, Phys. Rev. **17**, 2762 (1978).

[8] G. Zimmerer, in *Excited-State Spectroscopy in Solids*, edited by U. M. Grassano and N. Terzi (North-Holland, Amsterdam, 1987), p. 37.

[9] N. Schwentner, E. E. Koch, and J. Jortner, *Electronic Excitations in Condensed Rare Gases* (Springer-Verlag, Berlin, 1985).

[10] R. E. Johnson and M. Inokuti, Nucl. Instrum. Methods Phys. Res. **206**, 289 (1983).

[11] U. Sowada, J. M. Waman, and M. P. de Haas, Phys. Rev. B **25**, 3434 (1982).

[12] D. E. Grosjean, R. A. Baragiola, and W. L. Brown (to be published).

[13] F. Coletti, J. M. Debever, and G. Zimmerer, J. Phys. (France) Lett. **45**, L467 (1984).

[14] E. Morikawa, R. Reininger, P. Gürtler, V. Saile, and P. Laporte, J. Chem. Phys. **91**, 1469 (1989).

[15] F. Besenbacher, J. Bottiger, O. Graverson, and J. L. Hansen, Nucl. Instrum. Methods Phys. Res. **191**, 221 (1981).

[16] R. E. Johnson and J. Schou, Mat. Fys. Medd. K. Dan. Vidensk. Selsk. **43**, 403 (1993).

[17] C. T. Reimann, W. L. Brown, D. E. Grosjean, M. J. Nowakowski, W. T. Buller, S. Cui, and R. E. Johnson, Nucl. Instrum. Methods Phys. Res. B **58**, 404 (1991).

[18] A. Hitachi, T. Doke, and A. Mozumder, Phys. Rev. B **46**, 11 463 (1992).

[19] J. A. LaVerne, A. Hitachi, and T. Doke, Nucl. Instrum. Methods Phys. Res. A **327**, 63 (1993).

[20] S. Kubota, M. Hishida, M. Suzuki, and J. Ruan(Gen), Phys. Rev. B **20**, 3486 (1979).

[21] D. E. Grosjean, Ph.D. thesis, University of Virginia, 1996.

[22] G. Haas and W. R. Hunter, J. Quant. Spectrosc. Radiat. Transf. **2**, 637 (1962).

[23] A. Kouchi and T. Kuroda, Jpn. J. Appl. Phys. 2, Lett. **29**, L807 (1990).

[24] M. S. Westley, MSc. thesis, University of Virginia, 1994.

[25] C. T. Reimann, W. L. Brown, D. E. Grosjean, and M. J. Nowakowski, Phys. Rev. B **45**, 43 (1992).

[26] I. Ya. Fugol, Adv. Phys. **27**, 1 (1978).

[27] A. Hourmatallah, F. Coletti, and J. M. Debever, J. Phys. C **21**, 1307 (1988).

[28] E. E. Huber, Jr., D. A. Emmons, and R. M. Lerner, Opt. Commun. **11**, 155 (1974).

[29] Yu. B. Poltoratskii and I. Ya. Fugol, Sov. J. Low Temp. Phys. **4**, 373 (1979).

[30] H. Langhoff, Opt. Commun. **68**, 31 (1988).

[31] O. N. Grigorashchenko, S. A. Gubin, A. N. Ogurtsov, and E. V. Savchenko, J. Electron Spectrosc. Relat. Phenom. **79**, 107 (1996).

[32] M. Kraas and P. Gürtler, Chem. Phys. Lett. **174**, 396 (1990).

[33] A. Harmsen, E. E. Koch, V. Saile, N. Schwentner, and M. Skibowski, in *Vacuum Ultraviolet Radiation Physics*, edited by E. E. Koch, R. Haensel, and C. Kunz (Pergamon, New York, 1974), p. 339.

[34] J. F. Ziegler, J. P. Biersack, and U. Littmark, *The Stopping and Range of Ions in Solids*, (Pergamon, Oxford, 1985), Vol. 1.

[35] H. R. Philipp and E. A. Taft, Phys. Rev. **120**, 37 (1960).

[36] T. E. Stewart, G. S. Hurst, T. E. Bortner, J. E. Parks, F. W. Martin, and H. L. Weidner, J. Opt. Soc. Am. **60**, 1290 (1970).

[37] C. T. Reimann, Ph.D. thesis, University of Virginia, 1986.

[38] J. D. Jackson, *Classical Electrodynamics*, 2nd ed. (Wiley, New York, 1975), p. 278–82.

[39] G. B. Irani, T. Huen, and F. Wooten, J. Opt. Soc. Am. **61**, 128 (1971).

[40] H.-J. Hagemann, W. Gudat, and C. Kunz (unpublished).